Transplantation of Bone Marrow-Derived Very Small Embryonic-Like Stem Cells Attenuates Left Ventricular Dysfunction and Remodeling After Myocardial Infarction

Buddhadeb Dawn[a], **Sumit Tiwari**[a], **Magdalena J. Kucia**[b], **Ewa K. Zuba-Surma**[b], **Yiru Guo**[a], **Santosh K. SanganalMath**[a], **Ahmed Abdel-Latif**[a], **Greg Hunt**[a], **Robert J. Vincent**[a], **Hisham Taher**[a], **Nathan J. Reed**[a], **Mariusz Z. Ratajczak**[b], and **Roberto Bolli**[a]

[a]Institute of Molecular Cardiology, University of Louisville, Louisville, Kentucky, USA

[b]Stem Cell Biology Program, University of Louisville, Louisville, Kentucky, USA

Abstract

Adult bone marrow (BM) contains Sca-1+/Lin−/CD45− very small embryonic-like stem cells (VSELs) that express markers of several lineages, including cardiac markers, and differentiate into cardiomyocytes in vitro. We examined whether BM-derived VSELs promote myocardial repair after a reperfused myocardial infarction (MI). Mice underwent a 30-minute coronary occlusion followed by reperfusion and received intramyocardial injection of vehicle ($n = 11$), 1×10^5 Sca-1+/Lin−/CD45+ enhanced green fluorescent protein (EGFP)-labeled hematopoietic stem cells ($n = 13$ [cell control group]), or 1×10^4 Sca-1+/Lin−/CD45− EGFP-labeled cells ($n = 14$ [VSEL-treated group]) at 48 hours after MI. At 35 days after MI, VSEL-treated mice exhibited improved global and regional left ventricular (LV) systolic function (echocardiography) and attenuated myocyte hypertrophy in surviving tissue (histology and echocardiography) compared with vehicle-treated controls. In contrast, transplantation of Sca-1+/Lin−/CD45+ cells failed to confer any functional or structural benefits. Scattered EGFP+ myocytes and capillaries were present in the infarct region in VSEL-treated mice, but their numbers were very small. These results indicate that transplantation of a relatively small number of CD45− VSELs is sufficient to improve LV function and alleviate myocyte hypertrophy after MI, supporting the potential therapeutic utility of these cells for cardiac repair.

Keywords

Myocardial infarction; Myocardial regeneration; Very small embryonic-like stem cell; Stem cell; Bone marrow; Left ventricular function

Correspondence: Buddhadeb Dawn, M.D., Institute of Molecular Cardiology, University of Louisville, Louisville, Kentucky 40292, USA. Telephone: 502-852-7959; Fax: 502-852-7147; buddha@louisville.edu; Roberto Bolli, M.D., Institute of Molecular Cardiology, University of Louisville, Louisville, Kentucky 40292, USA. Telephone: 502-852-1837; Fax: 502-852-6474; rbolli@louisville.edu.

Disclosure of Potential Conflicts of Interest

The authors indicate no potential conflicts of interest.

Introduction

Numerous studies in animals have documented improvement in left ventricular (LV) function and anatomy following bone marrow cell (BMC) therapy after myocardial infarction (MI) [1]. The initial results of clinical trials also suggest improvement in LV function and reduction in scar size with BMC therapy in patients with acute MI, as well as ischemic cardiomyopathy [2]. However, several different BMC types, numbers, and routes of administration have been used in studies in animals and humans; the BMCs responsible for the salubrious effects of bone marrow (BM), as well as the ideal BMCs for cardiac repair, remain to be identified. In addition, the mechanisms underlying the benefits associated with BMC therapy remain poorly understood.

Although embryonic stem cells (ESCs) have been used in animal studies of cardiac repair [3, 4], ethical and regulatory issues limit the potential therapeutic utility of ESCs for cardiac repair in humans. Moreover, because of their pluripotent nature, transplanted ESCs may give rise to teratomas in vivo [5–7]. Because of these risks inherent in ESC therapy, we have directed our efforts to identifying an adult tissue-derived cell type with broader differentiation potential. We have recently reported that the adult BM contains a population of small CXCR4+ cells that are nonhematopoietic and express markers of lineage commitment for several different tissues, thereby exhibiting the potential to differentiate into various unrelated lineages [8–10]. These very small embryonic-like stem cells (VSELs) are Sca-1+/Lin−/CD45−; they express (among other lineage markers) cardiac markers, including Nkx2.5/Csx, GATA-4, and MEF2C, and acquire a cardiomyocytic phenotype in vitro under specific culture conditions [10]. We hypothesized that VSELs may account, at least in part, for the beneficial effects observed with BMC therapy in MI. We reasoned that if this thesis is correct, then selective administration of VSELs should be sufficient in itself to produce a functional and structural improvement in experimental MI, despite the absence of all of the other cell types present in the BM.

Accordingly, the goals of the present study were as follows: (a) to determine whether direct intramyocardial transplantation of VSELs results in improvement in LV function and postinfarct remodeling, and (b) to investigate the potential mechanisms underlying the effects of VSEL therapy. To separate cell-specific from nonspecific actions, Sca-1+/Lin−/CD45− VSELs were directly compared with Sca-1+/Lin−/CD45+ cells, which are highly enriched in hematopoietic stem cells and differ from VSELs only with respect to CD45 expression. The results show that administration of small numbers of VSELs after a reperfused MI is sufficient to improve LV function and dimensions and to attenuate cardiomyocyte hypertrophy. In contrast, transplantation of much larger numbers of Sca-1+/Lin−/CD45+ cells had no beneficial effect. The ability of VSELs to alleviate postinfarction LV remodeling warrants further investigation of the therapeutic utility of these cells and may have significant implications for the design of future studies of BMC-mediated cardiac repair both in animals and in humans.

Materials and Methods

The present study was performed in accordance with the guidelines of the Animal Care and Use Committee of the University of Louisville School of Medicine and with the Guide for the Care and Use of Laboratory Animals (Department of Health and Human Services, publication no. [NIH] 86-23).

Animals

A total of 233 mice (73 wild-type [WT] and 160 enhanced green fluorescent protein [EGFP] transgenic) were used. Sixty-six WT mice were assigned to the myocardial infarction studies (groups I–III), 160 EGFP transgenic mice were used as BM donors for cell isolation, and 7 noninfarcted mice were used for the determination of myocyte area.

Experimental Protocol

This study was performed in a well-established murine model of MI [11, 12]. The experimental protocol is summarized in supplemental online Figure 1. All mice (groups I–III) underwent a 30-minute coronary occlusion followed by 35 days of reperfusion. At 48 hours after reperfusion, mice received an intramyocardial injection of vehicle (group I), CD45+ hematopoietic stem cells (group II), or VSELs (group III). Echocardiographic studies were performed 4 days prior to coronary occlusion/reperfusion, 48 hours after cell injection (i.e., 96 hours after MI), and 35 days after MI (prior to sacrifice).

Isolation of VSELs and Sca-1+/Lin−/CD45+ Hematopoietic Stem Cells

VSELs and CD45+ cells were isolated as previously described [10]. Briefly, BMCs were obtained from the femur and tibia of 4–6-week-old male EGFP transgenic mice and red blood cells were lysed with a 0.9% solution of NH_4Cl. Freshly isolated BMCs were resuspended in phosphate-buffered saline (PBS) containing 1% fetal bovine serum (FBS; HyClone, Logan, UT, http://www.hyclone.com). The following primary antibodies were added simultaneously: biotin-conjugated monoclonal rat anti-mouse Ly-6A/E (Sca-1) (clone E13-161.7), APC-Cy7-conjugated monoclonal rat anti-mouse CD45 (clone 30-F11), and phycoerythrin (PE)-conjugated monoclonal rat anti-mouse lineage markers (anti-CD45R/B220 [PE; clone RA3-6B2], anti-Gr-1 [PE; clone RB6-8C5], anti-TCR$\alpha\beta$ [PE; clone H57-597], anti-TCR$\gamma;\delta$ [PE; clone GL3], anti-CD11b [PE; clone M1/70], anti-Ter119 [PE; clone TER-119]). Secondary staining was performed using PE-Cy5-conjugated streptavidin. All reagents were purchased from BD Pharmingen (San Jose, CA, http://www.bdbiosciences.com/index_us.shtml). Staining was performed at 4°C for 20 minutes, and cells were washed with PBS supplemented with 1% FBS after staining. Flow cytometric cell sorting was performed using a MoFlo machine (Dako, Carpinteria, CA, http://www.dako.com) according to the scheme presented in Figure 1. Bulk-sorted cells were collected into 2 ml of Dulbecco's modified Eagle's medium (DMEM) with 10% FBS. The purity was assessed by reanalyzing isolated cells immediately following sorting. The viability of sorted cells always exceeded 90%. Sorted cells were pelleted via centrifugation at 1,000g for 10 minutes and resuspended in DMEM with 10% FBS in a smaller volume proportional to cell number. Cells were aliquoted in a 50-μl volume for intramyocardial injection (total dose, 100,000 cells for group II and 10,000 cells for group III).

Myocardial Infarction and Cell Transplantation

Three groups of WT mice (C57/BL6 strain; body weight, 20–25 g; age, 10–12 weeks; Jackson Laboratory, Bar Harbor, ME, http://www.jax.org) were used. The experimental preparation has been described in detail [11, 12]. Mice were anesthetized with pentobarbital sodium (50 mg/kg i.p.), intubated, and ventilated using a small rodent ventilator. Body temperature, heart rate, and arterial pH were carefully maintained within the physiological range throughout the experiments. Using a sterile technique, the chest was opened through a midline sternotomy. An 8-0 nylon suture was passed with a tapered needle under a branch of the left coronary artery perfusing the mid-distal anterior wall and the apex at 2 mm from the tip of the left auricle, and a nontraumatic balloon occluder was applied on the artery. Coronary occlusion was induced by inflating the balloon occluder. Successful performance of coronary occlusion and reperfusion was verified by visual inspection (i.e., by noting the

development of a pale color in the distal myocardium upon inflation of the balloon and the return of a bright red color due to hyperemia after deflation) and by observing S-T segment elevation and widening of the QRS on the ECG during ischemia and their resolution after reperfusion [11, 12]. The chest was then closed in layers, and a small catheter was left in the thorax for 10–20 minutes to evacuate air and fluids. The mice were removed from the ventilator, kept warm with heat lamps, given fluids (1.0–1.5 ml of 5% dextrose in water intraperitoneally), and allowed 100% oxygen via nasal cone. Forty-eight hours later, mice were reanesthetized and ventilated, and the chest was reopened via aseptic technique. Vehicle (50 μl; group I), Sca-1+/Lin–/CD45+ hematopoietic stem cells (100,000 cells in 50 μl; group II), or Sca-1+/Lin–/CD45– VSELs (10,000 cells in 50 μl; group III) were injected intramyocardially using a 30-gauge needle. A total of five injections were made in the peri-infarct region in a circular pattern, at the border between infarcted and noninfarcted myocardium. The chest was closed in layers, and the mice were allowed to recover as described above.

Echocardiographic Studies

Echocardiograms were obtained using an HDI 5000 SonoCT echocardiography machine (Philips Medical Systems, Bothell, WA, http://www.medical.philips.com) equipped with a 15–7 MHz linear broadband transducer and a 12–5 MHz phased array transducers [13]. The mice were anesthetized with pentobarbital (25 mg/kg i.p.). The anterior chest was shaved, and the mice were placed in the left lateral decubitus position. Using a rectal temperature probe, body temperature was carefully maintained close to 37.0°C with a heating pad throughout the study. Modified parasternal long-axis and parasternal short-axis views were used to obtain two-dimensional, M-mode, and spectral Doppler images [13]. Systolic and diastolic anatomic parameters were obtained from M-mode tracings at the mid-papillary level. LV volume was estimated by the Teichholz formula. LV mass was estimated by the area-length method. Images were analyzed off-line using the Prosolv data analysis software (version 2.5; Problem Solving Concepts, Inc., Indianapolis, http://www.prosolv.com) by an investigator who was blind to the treatment allocation.

Morphometric Analyses

At the end of the study, the thorax was opened, the abdominal aorta was cannulated, and the heart was arrested in diastole with KCl and $CdCl_2$, excised, and perfused retrogradely through the aorta with 10% neutral-buffered formalin. The right atrium was cut to allow drainage. The perfusion pressure was adjusted to match the mean arterial pressure. The LV chamber was filled with fixative from a pressure reservoir set at a height equivalent to the in vivo-measured LV end-diastolic pressure [13–15]. The LV was sectioned serially into four rings perpendicular to its longitudinal axis, processed, and embedded in paraffin. The infarct area fraction was calculated by computerized planimetry (Image-Pro Plus; Media Cybernetics, Carlsbad, CA, http://www.mediacy.com) of digital images of three Masson's trichrome-stained serial LV sections taken at 0.5–1.0 mm intervals along the longitudinal axis [13, 14]. The mid-section was used to measure LV diameter. The thickness of the infarct wall, septal wall, and posterior wall was calculated in serial sections and averaged [13, 14]. An average sarcomere length of 2.1 μm was used in all cases to correct the raw measurements of LV anatomical parameters [15].

For the assessment of cardiomyocyte cross-sectional area, digital images were acquired from trichrome-stained myocardial sections. Cardiomyocyte cross-sectional area was measured in transversely sectioned myocytes with a circular profile and a central nucleus [16, 17]. We compared the three infarcted groups (groups I–III) with a separate control group of noninfarcted mice that were of similar age (10–12 weeks) and did not undergo surgery. On average, a total of 100 myocytes were measured in each heart. To assess the effect of cell

therapy on infarct repair, the area occupied by myocytes in the infarct zone was measured and expressed as a percentage of the total infarct area. (The infarct area was defined as the entire segment of LV that contained scar in myocardial sections stained with Masson's trichrome.) All morphometric analyses were performed by investigators who were blind to the treatment allocation.

Immunohistochemistry

Immunohistochemistry was performed in formalin-fixed 4-μm-thick histological sections. Cardiomyocytes were recognized by the presence of a-sarcomeric actin (Sigma-Aldrich, St. Louis, http://www.sigmaaldrich.com) and troponin T (Santa Cruz Biotechnology Inc., Santa Cruz, CA, http://www.scbt.com), endothelial cells by PECAM-1 (Santa Cruz Biotechnology) and von Willebrand factor (Sigma-Aldrich), and smooth muscle cells by a-smooth muscle actin (Sigma-Aldrich) [13, 18]. Colocalization of cell-specific markers with EGFP was used to identify cells that originated from BMCs [13, 19]. Nuclei were identified with 4,6-diamidino-2-phe-nylindole.

For the assessment of capillary density [16, 17], sections were stained with an anti-CD31 (Santa Cruz Biotechnology) primary antibody followed by the addition of a tetramethylrhodamine B isothiocyanate-conjugated secondary antibody [18]. CD31-positive capillary profiles were counted at a magnification of $\times100$ in contiguous fields in the infarct zone, border zone, and nonischemic zone. On average, a total of 40–50 fields were counted in each heart.

Statistical Analysis

Data are reported as mean $\pm$ SEM. Morphometric and histologic data were analyzed with a one-way analysis of variance (ANOVA), whereas serial echocardiographic parameters were analyzed with a two-way (time and group) ANOVA followed by Student's t tests with the Bonferroni correction as appropriate [20]. All statistical analyses were performed using the SPSS software (version 8; SPSS, Chicago, http://www.spss.com).

Results

Exclusions

Sixteen mice died in the early postinfarction period and nine mice died within 72 hours after intramyocardial injection. Three mice were excluded from the study because of failure of the coronary occluder, leaving a total of 11, 13, and 14 mice in groups I–III, respectively.

Myocardial Infarct Size

The average infarct area fraction did not differ significantly among the three groups (Fig. 2). The infarct area fraction measures the average area of scarred tissue, expressed as a percentage of the LV area in three LV sections 0.5–1.0 mm apart [13, 14, 17].

Transplantation of VSELs Attenuates LV Systolic Dysfunction

Before coronary occlusion (baseline), all parameters of LV function, measured by echocardiography, were similar in groups I, II, and III (Fig. 3). At 48 hours after cell transplantation (96 hours after reperfusion), the degree of LV systolic functional impairment was also similar among the groups (Fig. 3), indicating that the injury sustained during ischemia/reperfusion and that associated with intramyocardial injection were comparable. In vehicle-treated (group I) and CD45+ cell-treated (group II) mice, there was further functional deterioration between 96 hours and 35 days after reperfusion (Fig. 3G–3J). In contrast, in VSEL-treated mice (group III), neither global (Fig. 3G) nor regional (Fig. 3I, 3J)

LV systolic function was impaired at 35 days compared with 96 hours. As a result, at 35 days, mice in group III exhibited significantly greater LV ejection fraction (Fig. 3A–3G) and smaller LV end-systolic diameter (Fig. 3A–3F, 3H) compared with vehicle-treated (group I) and CD45+ cell-treated (group II) mice. In group III, there was also enhanced regional myocardial function in the infarct region, as evidenced by a 48% ($p < .05$) and 29% ($p < .05$) greater systolic infarct wall thickness (Fig. 3I) and a 44% ($p < .05$) and 21% greater systolic wall thickening fraction compared with groups I and II, respectively (Fig. 3A–3F, 3J).

Transplantation of VSELs Halts LV Remodeling

By morphometry, the average LV chamber diameter was 12% and 20% smaller in group III compared with groups I and II, respectively (p = not significant [NS] vs. group I; $p < .05$ vs. group II) (Fig. 4A–4D). The infarct wall thickness and the posterior LV wall thickness did not differ significantly among the three groups (Fig. 4E, 4G). The infarct wall thickness-to-chamber radius ratio was increased significantly in group III compared with group II ($p < .05$) (Fig. 4F). On average, the morphometrically estimated LV volume was 24% and 30% smaller in group III versus groups I and II, respectively (p = NS vs. group I; $p < .05$ vs. group II) (Fig. 4H). The echocardiographic measurements of LV diameter and volume at 35 days mirrored the trends observed by morphometry (supplemental online Fig. 2). In summary, both by morphometry and by echocardiography, there was a trend toward improvement in LV remodeling in VSEL-treated mice compared with vehicle-treated mice, but the differences were not statistically significant. No such trend was observed in CD45+ cell-treated mice (group II).

Transplantation of VSELs Attenuates LV Hypertrophy

Compared with noninfarcted control mice, the cross-sectional myocyte area was significantly increased both in vehicle-treated and in CD45+ cell-treated mice (228 ± 16 μm^2 [+41%] and 258 ± 17 μm^2 [+59%] in groups I and II, respectively, vs. 162 ± 20 μm^2 in noninfarcted controls; $p < .05$ for both) (Fig. 5). In contrast, in VSEL-treated mice (group III), the myocyte area did not differ from that of noninfarcted mice (Fig. 5). The myocyte area in group III was 15% (P = NS) and 30% ($p < .05$) smaller, respectively, than in groups I and II (Fig. 5). These results were corroborated by the echocardiographic estimates of LV mass. Although at 35 days after MI the echocardiographically estimated LV mass was significantly increased in all groups compared with baseline values, in VSEL-treated mice the LV mass was 28% smaller than in groups I and II (123 ± 7 mg vs. 172 ± 14 and 170 ± 6 mg, respectively; $p < .05$ for both) (Fig. 5). Taken together, these data indicate that transplantation of VSELs is associated with attenuation of myocyte hypertrophy in surviving tissue.

Impact of VSEL Therapy on Viable Myocardium in the Scar

Scattered EGFP+ cardiomyocytes were identified in the infarct zone in group III (Fig. 6), whereas none were observed in group II; the number of EGFP+ myocytes, however, was extremely small. Myocytes constituted 52.9% $\pm$ 3.3%, 46.5% $\pm$ 2.9%, and 60.6% $\pm$ 2.3% of the infarct zone in groups I, II, and III, respectively (Fig. 7); therefore, the amount of viable myocardium in the infarct zone was, on average, 15% and 30% greater in VSEL-treated mice compared with vehicle-treated and CD45+ cell treated mice, respectively (P = NS vs. vehicle; $p < .05$ vs. CD45+ cells).

Impact of Cell Therapy on Capillary Density, Myocyte Apoptosis, and Myocyte Cycling

There was no significant difference among the three groups in myocardial capillary density in the infarct border zone and in the nonischemic zone (supplemental online Fig. 3). Similarly, in either zone there was no significant difference among the three groups with

respect to immunoreactivity for hairpin-1 probe (for the detection of apoptosis) and Ki67 (a marker of cell cycling) (data not shown).

Discussion

BMCs represent a heterogeneous population that includes various stem/progenitor cells with diverse differentiation potentials. Although mounting evidence supports the concept that BMC therapy promotes cardiac repair, the mechanisms underlying these beneficial effects remain controversial. We have previously proposed that adult BM cells predestined to differentiate into various lineages (VSELs) might be responsible for the formation of tissue-specific cells after BMC transplantation [8–10]—a concept that would reconcile the controversy regarding "plasticity" and "transdifferentiation" of BMCs [21, 22]. As an initial test of this theory, in the present study we examined the ability of VSELs to improve LV function and anatomy after a reperfused MI.

The major findings of the present study can be summarized as follows: (a) myocardial transplantation of only 10,000 VSELs after a reperfused MI is sufficient to induce a demonstrable improvement in LV function and dimensions; (b) this salubrious effect was associated with attenuation of LV hypertrophy in the noninfarcted region and the presence of regenerated myocytes derived from VSELs, although the number of these myocytes was very small; and (c) in contrast, transplantation of a 10-fold greater number of Sca-1+/Lin−/CD45+ hematopoietic stem cells did not improve LV function and dimensions. These results demonstrate that even a relatively small number of BM cells with robust differentiation potential can confer cardiac reparative benefits, whereas a much greater number of CD45+ hematopoietic stem cells fails to do so. The observations reported here underscore the importance of proper selection of BM cells and support the concept that small quantities of VSELs present in the transplanted BM preparations may account for the beneficial effects previously observed after BMC therapy [2, 23, 24]. Collectively, our findings have important conceptual implications for our understanding of BM-dependent cardiac repair and provide a rationale for further studies aimed at optimizing cell therapy by selective use of BM-derived VSELs.

Cardiac repair via cellular transplantation has generated considerable enthusiasm in recent years. Although the optimal cell for cardiac repair remains to be identified, pluripotent ESCs have been used for this purpose in several laboratories [3, 4]. However, the therapeutic use of ESCs for cardiac repair in humans is fraught with ethical and regulatory concerns. Besides, it is unclear whether ESCs indeed differentiate into cardiomyocytes following transplantation. In a recent study [5], investigators failed to identify cardiomyocytes of human origin following transplantation of human ESCs and embryoid bodies into infarcted hearts of athymic nude rats. In addition, transplantation of human ESC-derived cardiomyocytes may result in teratoma formation [5]. Teratoma formation following ESC transplantation has also been documented by several other investigators [6, 7]. In view of these concerns and risks associated with ESC therapy, we investigated the utility of cells that are harvested from adult tissues yet possess greater differentiation potential for cardiac repair in vivo.

The major controversial issue regarding the mechanism of BMC-based therapies is whether adult BM cells differentiate into cardiac and vascular lineages. We have previously reported the existence of small CXCR4+ cells within the adult BM that express markers indicative of commitment to several different lineages, including endothelial, skeletal muscle, neuronal, and cardiac lineages [8–10]. In view of the ability of VSELs to differentiate into cells with cardiomyocytic and endothelial phenotypes in vitro, we postulated that transplantation of VSELs after MI would improve cardiac function and LV remodeling. The present study

supports our working hypothesis, since it demonstrates that administration of a mere 10,000 VSELs results in amelioration of LV function and attenuation of LV dilation. The magnitude of these beneficial effects was modest, possibly because of the small number of VSELs injected. Larger numbers of VSELs could not be procured because these cells are rare (there is approximately 1 VSEL for 10,000 BM mononuclear cells [10]), and at the time of this investigation, we were unable to expand them in vitro. To inject 10,000 VSELs into one heart, we had to use the entire amount of BM collected from 3–4 EGFP transgenic mice (a total of 160 EGFP transgenic mice were used for this study). Previous investigators using BMCs [25–28] injected 10–100-fold greater numbers of cells (1×10^5 to 1×10^6 cells) into the infarcted murine heart. It is conceivable that transplantation of similar numbers of VSELs could result in greater effects than those observed in this study with 10,000 VSELs. We are currently developing methods for in vitro expansion of VSELs, which will enable us to assess the dose dependence of VSEL therapy.

Because several different cell types have been reported to be beneficial, there is a perception that any cell therapy can alleviate postinfarction LV remodeling. Therefore, we felt it was important to compare the effects of VSELs (which are Sca-1+, Lin−, CD45−, and nonhematopoietic) not only with vehicle but also with another cell type. We chose Sca-1+/Lin−/CD45+ hematopoietic stem cells because the only difference between these two cell populations is CD45 expression; thus, Sca-1+/Lin−/CD45+ cells are perhaps the best control cells for studying the actions of VSELs. Because of their Sca-1-positive and lineage-negative nature, Sca-1+/Lin−/CD45+ cells are highly purified bona fide primitive cells that are enriched in hematopoietic stem cells; therefore, this "control" subpopulation is very unlikely to contain any cell type (for example, macrophages, fibroblasts, leukocytes, etc.) that might have potentially exerted adverse effects on the myocardium after transplantation. To ensure that a salubrious effect of the CD45+ cells would not be missed, and to strengthen the evidence supporting the beneficial actions of VSELs, we decided to transplant CD45+ cells at a 10-fold greater number than VSELs. (The supply of CD45+ cells is not limited by the constraints described above for VSELs.) We reasoned that if CD45+ cells have the potential to promote cardiac repair, transplantation of only 10,000 such cells might not be sufficient to detect this property. Furthermore, by comparing 100,000 CD45+ cells with 10,000 VSELs, we "biased" the experiment in favor of CD45+ cells, so that any evidence favoring the superiority of VSELs would be much stronger. In this regard, it is important to note that the results of studies that examined the relationship between cell dose and efficacy of cardiac repair following cell transplantation indicate that the benefits of cell therapy are more pronounced when a greater number of cells are transplanted. This dose-dependent increase in benefits has been observed with bone marrow mononuclear cells (BMMNCs) [29], as well as with more purified CD34+ cell populations [30, 31]. In a study that compared unfractionated BMMNCs versus purified CD34+ cells, Kawamoto et al. [32] noted an increased incidence of hemorrhagic infarcts with a higher dose of BMMNCs; however, the outcomes (capillary density, percentage of fibrosis, and myocardial function) were marginally better, and certainly not worse, in the high-dose BMMNC group compared with the vehicle and low-dose BMMNC groups [32]. These reports, combined with the fact that a highly purified stem cell population was used as "control" in our study, suggest that the worse outcome in group II could not be ascribed to the greater cell number. Indeed, our finding that the transplantation of CD45+ cells did not favorably affect any of the measures of LV function and remodeling provides assurance that the beneficial effects observed with 10-fold lower numbers of VSELs were the result of genuine reparative properties rather than a nonspecific effect of cell therapy.

The mechanism that underlies the improvement in postinfarction remodeling after transplantation of VSELs remains unclear. Isolated new cardiomyocytes and capillaries derived from the EGFP-labeled VSELs were observed in the infarct region, but their number

was too small to account for the beneficial effects observed. VSELs may inhibit myocyte apoptosis and/or activate endogenous cardiac stem cells [33, 34], resulting in preservation of cardiac mass and/or new myocyte formation. Although our measurements of hairpin-1 and Ki67 positivity did not differ among the three groups at 35 days after MI, it remains possible that VSEL therapy was associated with reduction of apoptosis and/or increased cell cycling at earlier time points. It is also possible that secretion of growth factors by VSELs might inhibit hypertrophy, which would be expected to have favorable consequences on LV function. This is supported by the attenuated cardiomyocyte hypertrophy found in VSEL-treated hearts (Fig. 5). On the other hand, the opposite is also possible, that is, the inhibition of hypertrophy in VSEL-treated mice might have been the consequence (rather than the cause) of an improvement in LV function induced by VSELs via other mechanisms. Additional studies will be necessary to test these hypotheses. Whatever the mechanism for the effects of VSELs, it seems reasonable to postulate that it would be potentiated by the transplantation of greater numbers of these cells.

The present results have implications for BMC-mediated cardiac repair. Our data indicate that CD45− nonhematopoietic VSELs are more effective than CD45+ hematopoietic stem cells, and it seems plausible that an even more substantial improvement in LV function and structure after MI would be achieved with greater numbers of VSELs. Furthermore, the present observations imply that VSELs are at least one of the specific subtype(s) of BMCs that account for the beneficial effects observed in several experimental and clinical studies of BMC transplantation [2, 23, 24, 35]. This suggests that selective administration of expanded VSELs may be more effective than unfractionated BM transplantation. Since VSELs are normally present in the adult BM [10], harvest and transplantation of these cells can potentially be accomplished in humans. In view of these considerations, further experimental and clinical investigation of the therapeutic utility of VSELs appears to be in order.

Conclusion

We have provided proof of concept that BM-derived VSELs can be used to alleviate LV remodeling after MI. Transplantation of a relatively small number of VSELs was sufficient to improve LV function and alleviate myocyte hypertrophy. The mechanism remains uncertain, but it cannot consist solely of regeneration of VSEL-derived cardiomyocytes. In contrast, transplantation of a 10-fold greater number of CD45+ hematopoietic stem cells was ineffective, underscoring the specificity of the actions of VSELs. Taken together, the present results expand our previous studies of VSELs [9, 10] and support the concept that VSEL transplantation could be used therapeutically for cardiac repair after MI. Future investigations will be necessary to elucidate the mechanism(s) underlying VSEL-mediated improvement in postinfarction LV remodeling and to determine the efficacy of greater doses of VSELs.

Supplementary Material

Refer to Web version on PubMed Central for supplementary material.

Acknowledgments

References

1. Bolli R, Jneid H, Dawn B. Bone marrow cell-mediated cardiac regeneration a veritable revolution. J Am Coll Cardiol. 2005; 46:1659–1661. [PubMed: 16256865]

2. Abdel-latif A, Bolli R, Tleyjeh IM, et al. Adult bone marrow-derived cells for cardiac repair: A systematic review and meta-analysis. Arch Int Med. 2007; 167:989–997. [PubMed: 17533201]

3. Min JY, Yang Y, Converso KL, et al. Transplantation of embryonic stem cells improves cardiac function in postinfarcted rats. J Appl Physiol. 2002; 92:288–296. [PubMed: 11744672]

4. Kofidis T, de Bruin JL, Yamane T, et al. Insulin-like growth factor promotes engraftment, differentiation, and functional improvement after transfer of embryonic stem cells for myocardial restoration. Stem Cells. 2004; 22:1239–1245. [PubMed: 15579642]

5. Leor J, Gerecht S, Cohen S, et al. Human embryonic stem cell transplantation to repair the infarcted myocardium. Heart. 2007; 93:1278–1284. [PubMed: 17566061]

6. Swijnenburg RJ, Tanaka M, Vogel H, et al. Embryonic stem cell immunogenicity increases upon differentiation after transplantation into ischemic myocardium. Circulation. 2005; 112:I166–I172. [PubMed: 16159810]

7. Nussbaum J, Minami E, Laflamme MA, et al. Transplantation of undifferentiated murine embryonic stem cells in the heart: Teratoma formation and immune response. FASEB J. 2007; 21:1345–1357. [PubMed: 17284483]

8. Ratajczak MZ, Kucia M, Reca R, et al. Stem cell plasticity revisited: CXCR4-positive cells expressing mRNA for early muscle, liver and neural cells 'hide out' in the bone marrow. Leukemia. 2004; 18:29–40. [PubMed: 14586476]

9. Kucia M, Dawn B, Hunt G, et al. Cells expressing early cardiac markers reside in the bone marrow and are mobilized into the peripheral blood following myocardial infarction. Circ Res. 2004; 95:1191–1199. [PubMed: 15550692]

10. Kucia M, Reca R, Campbell FR, et al. A population of very small embryonic-like (VSEL) CXCR4(+)SSEA-1(+)Oct-4+ stem cells identified in adult bone marrow. Leukemia. 2006; 20:857–869. [PubMed: 16498386]

11. Guo Y, Wu WJ, Qiu Y, et al. Demonstration of an early and a late phase of ischemic preconditioning in mice. Am J Physiol. 1998; 275:H1375–H1387. [PubMed: 9746488]

12. Guo Y, Jones WK, Xuan YT, et al. The late phase of ischemic preconditioning is abrogated by targeted disruption of the inducible NO synthase gene. Proc Natl Acad Sci U S A. 1999; 96:11507–11512. [PubMed: 10500207]

13. Dawn B, Guo Y, Rezazadeh A, et al. Postinfarct cytokine therapy regenerates cardiac tissue and improves left ventricular function. Circ Res. 2006; 98:1098–1105. [PubMed: 16556872]

14. Li Q, Li B, Wang X, et al. Overexpression of insulin-like growth factor-1 in mice protects from myocyte death after infarction, attenuating ventricular dilation, wall stress, and cardiac hypertrophy. J Clin Invest. 1997; 100:1991–1999. [PubMed: 9329962]

15. Anversa, P.; Olivetti, G. The cardiovascular system. In: Page, E.; Fozzard, HA.; Solaro, RJ., editors. The Heart. 1. New York: Oxford University Press; 2002. p. 5-144.

16. Anversa P, Melissari M, Beghi C, et al. Structural compensatory mechanisms in rat heart in early spontaneous hypertension. Am J Physiol. 1984; 246:H739–H746. [PubMed: 6742139]

17. Anversa P, Beghi C, Kikkawa Y, et al. Myocardial infarction in rats. Infarct size, myocyte hypertrophy, and capillary growth. Circ Res. 1986; 58:26–37. [PubMed: 3943155]

18. Dawn B, Stein AB, Urbanek K, et al. Cardiac stem cells delivered intravascularly traverse the vessel barrier, regenerate infarcted myocardium, and improve cardiac function. Proc Natl Acad Sci U S A. 2005; 102:3766–3771. [PubMed: 15734798]

19. Orlic D, Kajstura J, Chimenti S, et al. Bone marrow cells regenerate infarcted myocardium. Nature. 2001; 410:701–705. [PubMed: 11287958]

20. Wallenstein S, Zucker CL, Fleiss JL. Some statistical methods useful in circulation research. Circ Res. 1980; 47:1–9. [PubMed: 7379260]

21. Dawn B, Bolli R. Adult bone marrow-derived cells: Regenerative potential, plasticity, and tissue commitment. Basic Res Cardiol. 2005; 100:494–503. [PubMed: 16237509]

22. Kucia M, Ratajczak J, Ratajczak MZ. Are bone marrow stem cells plastic or heterogenous–that is the question. Exp Hematol. 2005; 33:613–623. [PubMed: 15911085]

23. Strauer BE, Brehm M, Zeus T, et al. Repair of infarcted myocardium by autologous intracoronary mononuclear bone marrow cell transplantation in humans. Circulation. 2002; 106:1913–1918. [PubMed: 12370212]

24. Schächinger V, Erbs S, Elsasser A, et al. Intracoronary bone marrow-derived progenitor cells in acute myocardial infarction. N Engl J Med. 2006; 355:1210–1221. [PubMed: 16990384]

25. Toma C, Pittenger MF, Cahill KS, et al. Human mesenchymal stem cells differentiate to a cardiomyocyte phenotype in the adult murine heart. Circulation. 2002; 105:93–98. [PubMed: 11772882]

26. Yoon YS, Wecker A, Heyd L, et al. Clonally expanded novel multipotent stem cells from human bone marrow regenerate myocardium after myocardial infarction. J Clin Invest. 2005; 115:326–338. [PubMed: 15690083]

27. Kajstura J, Rota M, Whang B, et al. Bone marrow cells differentiate in cardiac cell lineages after infarction independently of cell fusion. Circ Res. 2005; 96:127–137. [PubMed: 15569828]

28. Wang Y, Haider HK, Ahmad N, et al. Combining pharmacological mobilization with intramyocardial delivery of bone marrow cells over-expressing VEGF is more effective for cardiac repair. J Mol Cell Cardiol. 2006; 40:736–745. [PubMed: 16603183]

29. Meluzin J, Mayer J, Groch L, et al. Autologous transplantation of mononuclear bone marrow cells in patients with acute myocardial infarction: The effect of the dose of transplanted cells on myocardial function. Am Heart J. 2006; 152:975.e9–e15. [PubMed: 17070173]

30. Schuster MD, Kocher AA, Seki T, et al. Myocardial neovascularization by bone marrow angioblasts results in cardiomyocyte regeneration. Am J Physiol Heart Circ Physiol. 2004; 287:H525–H532. [PubMed: 15277196]

31. Iwasaki H, Kawamoto A, Ishikawa M, et al. Dose-dependent contribution of CD34-positive cell transplantation to concurrent vasculogenesis and cardiomyogenesis for functional regenerative recovery after myocardial infarction. Circulation. 2006; 113:1311–1325. [PubMed: 16534028]

32. Kawamoto A, Iwasaki H, Kusano K, et al. CD34-positive cells exhibit increased potency and safety for therapeutic neovascularization after myocardial infarction compared with total mononuclear cells. Circulation. 2006; 114:2163–2169. [PubMed: 17075009]

33. Beltrami AP, Barlucchi L, Torella D, et al. Adult cardiac stem cells are multipotent and support myocardial regeneration. Cell. 2003; 114:763–776. [PubMed: 14505575]

34. Urbanek K, Rota M, Cascapera S, et al. Cardiac stem cells possess growth factor-receptor systems that after activation regenerate the infarcted myocardium, improving ventricular function and long-term survival. Circ Res. 2005; 97:663–673. [PubMed: 16141414]

35. Perin EC, Dohmann HF, Borojevic R, et al. Improved exercise capacity and ischemia 6 and 12 months after transendocardial injection of autologous bone marrow mononuclear cells for ischemic cardiomyopathy. Circulation. 2004; 110:II213–II218. [PubMed: 15364865]
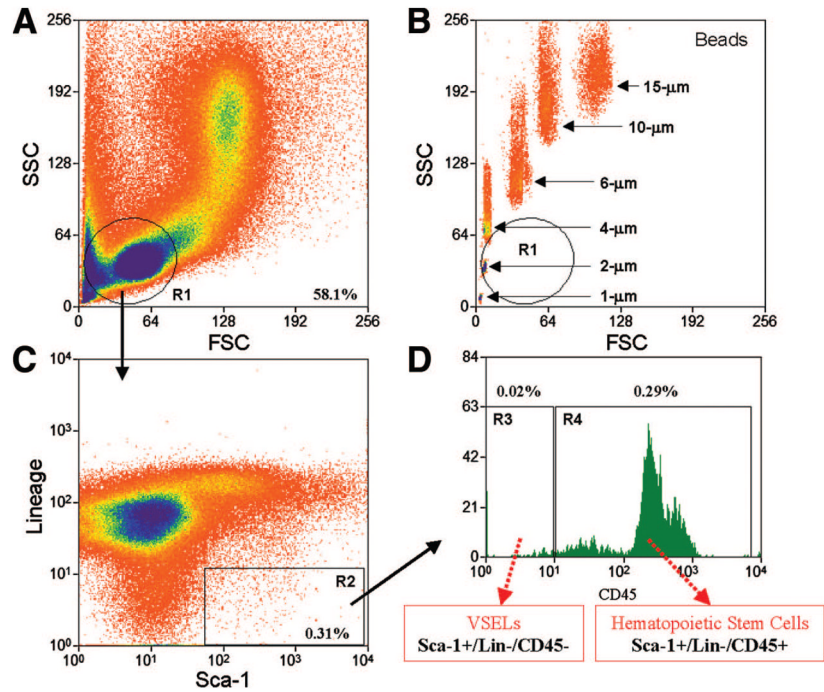
Figure 1.
Flow cytometric isolation of bone marrow-derived Sca-1+/Lin−/CD45+ hematopoietic stem cells and Sca-1+/Lin−/CD45− VSELs. Representative dot plots show sorting of small cells from the lymphoid gate **(A)** based on expression of Sca-1 (fluorescein isothiocyanate) and lineage markers (phycoerythrin) **(C)** and CD45 (APC-Cy7). **(D):** R3 contains Sca-1+/lin−/CD45− VSELs, whereas R4 contains Sca-1+/lin−/CD45+ cells. By comparing the sorting of bone marrow cells (BMCs) with the sorting of beads with known diameter, the FSC axis in **(B)** confirms the very small size (2–10 μm) of the cells in the region of interest in **(A)**. As shown here (R3), only 0.02% of total BMCs are VSELs. Abbreviations: FSC, forward scatter characteristics; R, region; SSC, side scatter characteristics; VSEL, very small embryonic-like stem cell.
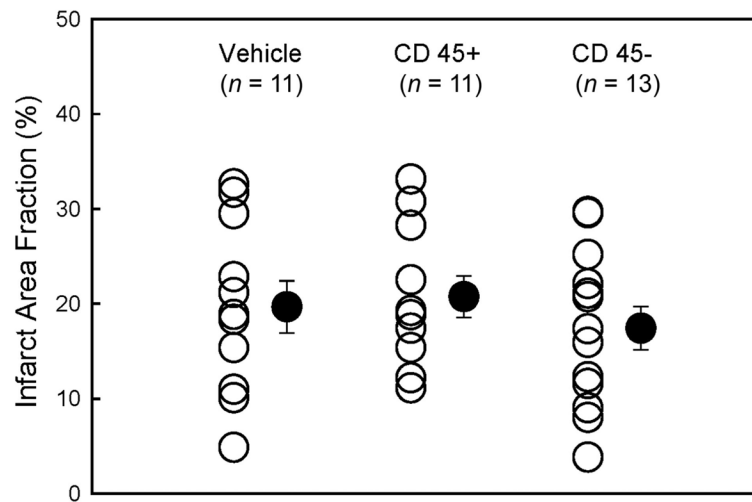
Figure 2.
Myocardial infarct size. Myocardial infarct area fraction ([infarct area/left ventricular area] × 100) assessed from Masson's trichrome-stained hearts in groups I–III, which were treated with vehicle, CD45+ hematopoietic stem cells, and very small embryonic-like stem cells, respectively. ○, individual mice; ●, mean ± SEM.
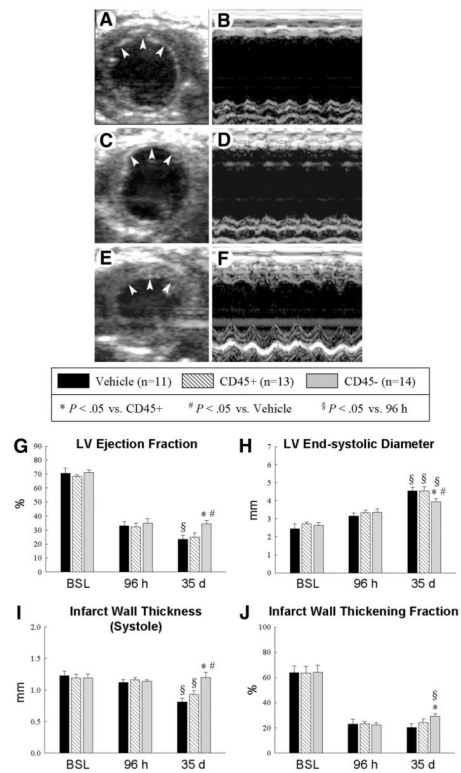
Figure 3.
Echocardiographic assessment of LV function. Representative two-dimensional **(A, C, E)** and M-mode **(B, D, F)** images from vehicle-treated **(A, B)**, CD45+ cell-treated **(C, D)**, and very small embryonic-like stem cell (VSEL)-treated **(E, F)** mice 35 d after coronary occlusion/reperfusion. The infarct wall is delineated by arrowheads **(A, C, E)**. Compared with the vehicle-treated and CD45+ cell-treated hearts, the VSEL-treated heart exhibited a smaller LV cavity, a thicker infarct wall, and improved motion of the infarct wall. Panels **(G–J)** demonstrate that transplantation of VSEL improved echocardiographic measurements of LV systolic function 35 d after myocardial infarction. Data are mean ± SEM. $n = 11$–14 mice per group. *, $p < .05$ versus group II at 35 d; #, $p < .05$ versus group I at 35 d; §, $p < .05$ versus values at 96 h in respective groups. Abbreviations: BSL, baseline; d, days; h, hours; LV, left ventricular.
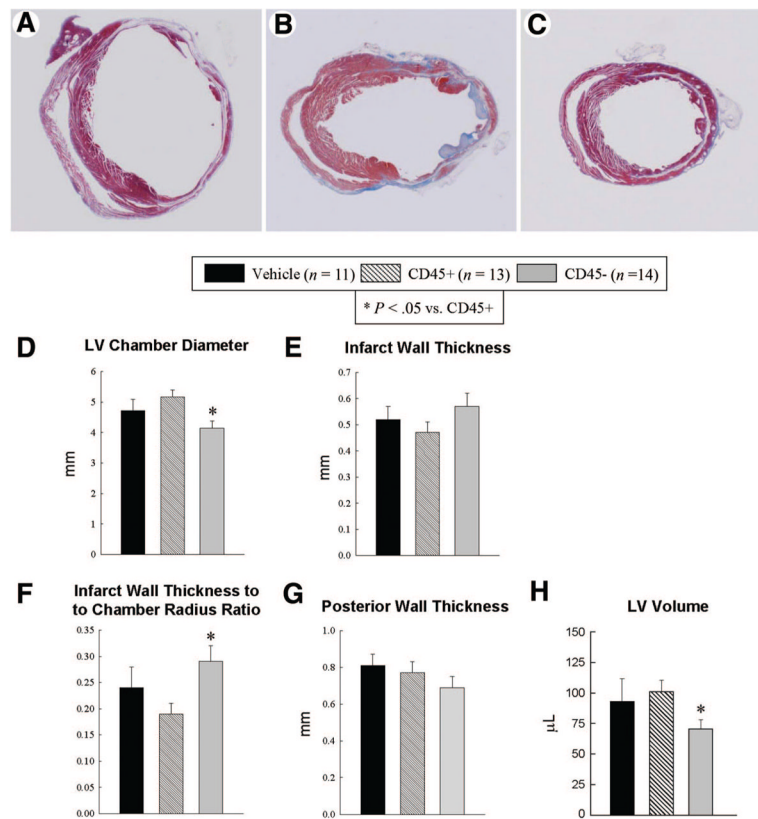
Figure 4.
Morphometric assessment of LV remodeling. Representative Masson's trichrome-stained myocardial sections from vehicle-treated **(A)**, CD45+ hematopoietic stem cell-treated **(B)**, and very small embryonic-like stem cell (VSEL)-treated **(C)** hearts. Scar tissue and viable myocardium are identified in blue and red, respectively. Note that the LV cavity is smaller and the infarct wall thicker in the VSEL-treated heart. Panels **(D–H)** illustrate morphometric measurements of LV structural parameters. Data are mean ± SEM. $n = 11$–14 mice per group. *, $p < .05$ versus group II. Abbreviation: LV, left ventricular.
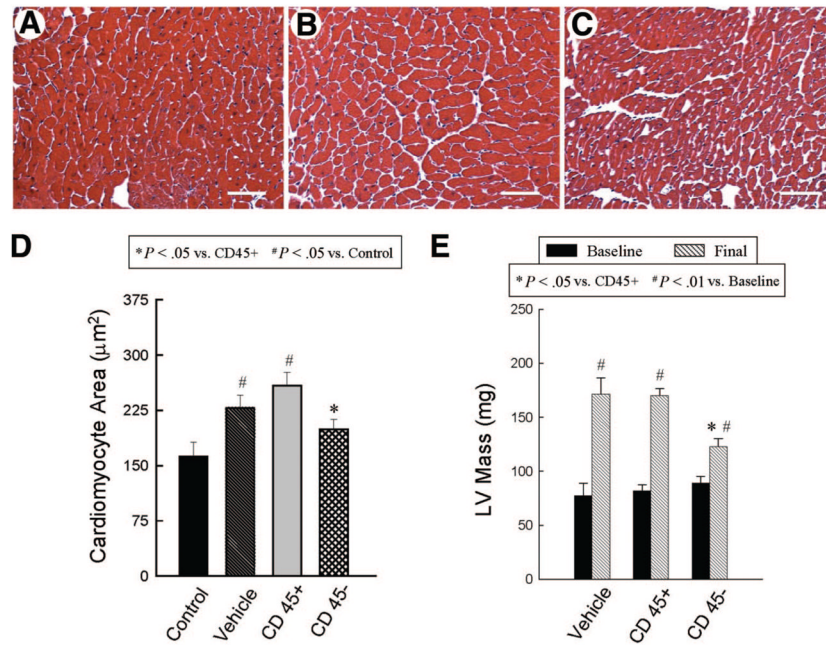
Figure 5.
Assessment of cardiomyocyte and LV hypertrophy. Panels **(A–C)** show representative images of cardiomyocytes in the viable myocardium from Masson's trichrome-stained vehicle-treated **(A)**, CD45+ hematopoietic stem cell-treated **(B)**, and very small embryonic-like stem cell (VSEL)-treated hearts **(C)**. Scale bars = 50 μm. In contrast to CD45+ hematopoietic stem cell-treated hearts, VSEL-treated hearts did not exhibit increased myocyte cross-sectional area compared with noninfarcted control hearts **(D)**. Echocardiographically estimated LV mass was significantly less in VSEL-treated hearts **(E)**. Data are mean ± SEM. n = 11–14 mice per group. **(D):** *, $p < .05$ versus group II; #, $p < .05$ versus control; **(E):** *, $p < .05$ versus group II and III (final); #, $p < .05$ versus respective baseline values. Abbreviation: LV, left ventricular.
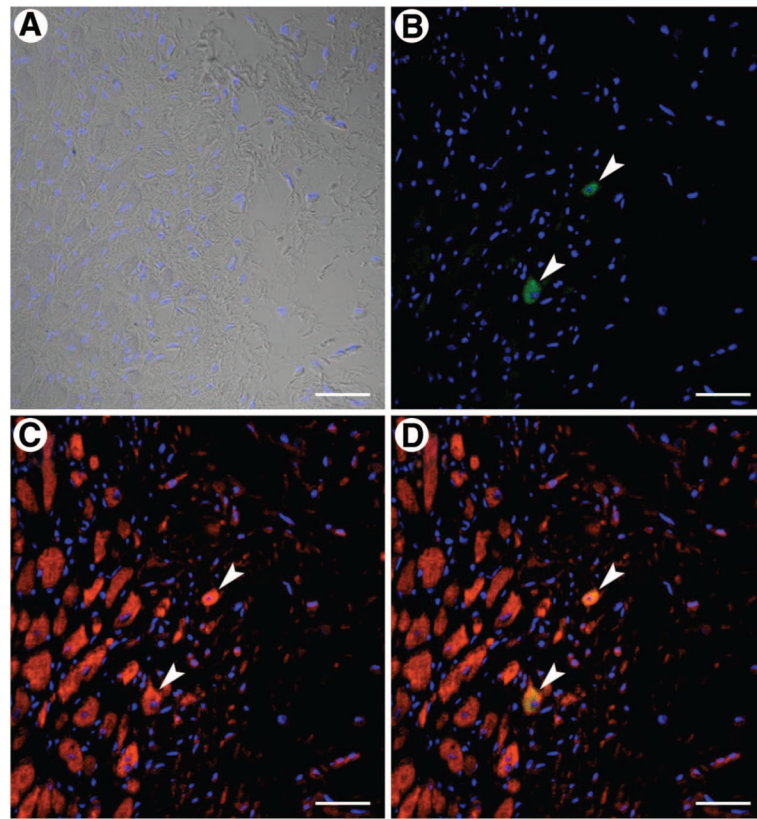
Figure 6.
Very small embryonic-like stem cell (VSEL) transplantation and cardiomyocyte regeneration. VSELs and myocytes are identified by enhanced green fluorescent protein (EGFP) ([**B, D**], green) and α-sarcomeric actin ([**C, D**], red), respectively; (**D**) shows the merged image. Two myocytes are shown that are positive for both EGFP (arrowheads; [**B**], green) and α-sarcomeric actin (arrowheads; [**C**], red). Nuclei were stained with 4,6-diamidino-2-phenylindole ([**A, D**], blue). Scale bars = 40 μm.
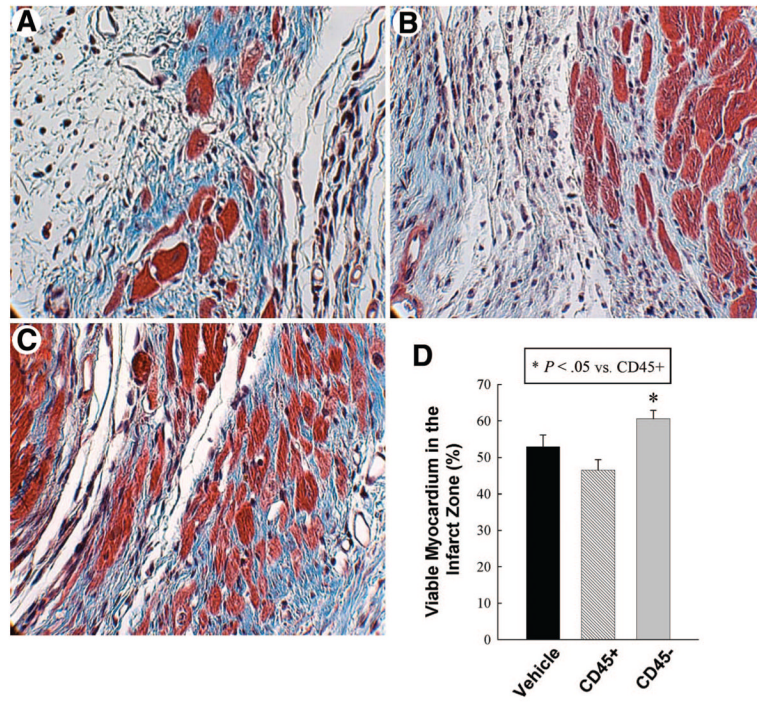
Figure 7.
Assessment of myocyte area fraction in the infarct area. Panels **(A–C)** illustrate representative examples of scar in Masson's trichrome-stained, vehicle-treated **(A)**, CD45+ hematopoietic stem cell-treated **(B)**, and very small embryonic-like stem cell-treated **(C)** hearts. Magnification, ×600. Quantitative data are presented in **(D)**. Data are mean ± SEM. *n* = 11–14 mice per group. *, *p* < .05 versus group II.